# A comparison of fibre-optic distributed temperature sensing to traditional methods of evaluating groundwater inflow to streams

Martin A. Briggs,[1]* Laura K. Lautz[1] and Jeffrey M. McKenzie[2]

[1] *Department of Earth Sciences, Syracuse University, 204 Heroy Geology Laboratory, Syracuse, NY 13244, USA*
[2] *Department of Earth and Planetary Sciences, McGill University, 3450 University Street, Montreal, PQ, Canada H3A 2A7*

## Abstract:

There are several methods for determining the spatial distribution and magnitude of groundwater inputs to streams. We compared the results of conventional methods [dye dilution gauging, acoustic Doppler velocimeter (ADV) differential gauging, and geochemical end-member mixing] to distributed temperature sensing (DTS) using a fibre-optic cable installed along 900 m of Ninemile Creek in Syracuse, New York, USA, during low-flow conditions (discharge of $1.4 \text{ m}^3 \text{ s}^{-1}$). With the exception of differential gauging, all methods identified a focused, contaminated groundwater inflow and produced similar groundwater discharge estimates for that point, with a mean of $66.8 \text{ l s}^{-1}$ between all methods although the precision of these estimates varied. ADV discharge measurement accuracy was reduced by non-ideal conditions and failed to identify, much less quantify, the modest groundwater input, which was only 5% of total stream flow. These results indicate ambient tracers, such as heat and geochemical mixing, can yield spatially and quantitatively refined estimates of relatively modest groundwater inflow even in large rivers. DTS heat tracing, in particular, provided the finest spatial characterization of groundwater inflow, and may be more universally applicable than geochemical methods, for which a distinct and consistent groundwater end member may be more difficult to identify. Copyright © 2011 John Wiley & Sons, Ltd.

KEY WORDS    groundwater–surface-water interaction; tracer tests; distributed temperature sensing; heat tracing

*Received 30 June 2010; Accepted 10 June 2011*

## INTRODUCTION

Groundwater enters streams as baseflow by passing across the streambed interface, a process that is governed by a complex combination of geomorphologic variables and hydraulic head gradients. Depending on the site-specific dissolved gasses, dissolved load, and temperature of groundwater inflow, these inputs often serve as a vital control on the water quality and stream ecology of gaining systems. During dry periods baseflow often maintains habitat and is the principal component of total stream discharge (Brunke and Gonser, 1997). Therefore, accurate evaluations of the spatial distribution and magnitudes of groundwater inflows to streams are of primary interest to researchers and water resource managers. This is particularly significant when determining dissolved mass inputs from groundwater influenced by point source contamination (Kalbus *et al.*, 2006). Many potential groundwater contaminants of interest are toxic in very low concentrations, yet inputs to large streams may be difficult to locate and quantify as they generally contribute only a small fraction of overall stream flow. There are several well-known field techniques available with which to evaluate groundwater inflows to streams, each with particular strengths and scale applicability.

Other researchers have compared and contrasted many of these traditional techniques (Zellweger, 1994; Fulford, 2001; Kalbus *et al.*, 2006; Soupir *et al.*, 2009), but we compare three of the most widely used with the new distributed temperature sensing (DTS) heat tracing method in a large stream influenced by contaminated groundwater to assess the repeatability, practicality, and spatial resolution of discharge estimates.

One of the most common methods of measuring groundwater inflows to streams is differential gauging, where the net change in stream flow between incremental stream cross-sections is determined. Discharge through a cross-section is estimated by the velocity gauging method (Carter and Davidian, 1968) for which total discharge is determined by multiplying representative velocity estimates by corresponding areas and summing over the section. Velocity point measurements are often made at representative depths (e.g. 6/10 of the total depth) with current meters consisting of rotating propellers or electromagnetic sensors. More recently, acoustic doppler devices have become available that measure flow in multiple dimensions (Soupir *et al.*, 2009) and may include integrated software packages to calculate discharge and assess error (e.g. SonTek/YSI, 2009). Another variant on this popular method of determining discharge at successive points is dilution gauging, for which an introduced conservative tracer, such as a salt or dye, is mixed with stream water and discharge is determined from successive

* Correspondence to: Martin A. Briggs, Department of Earth Sciences, Syracuse University, 204 Heroy Geology Laboratory, Syracuse, NY 13244, USA. E-mail: mabriggs@syr.edu
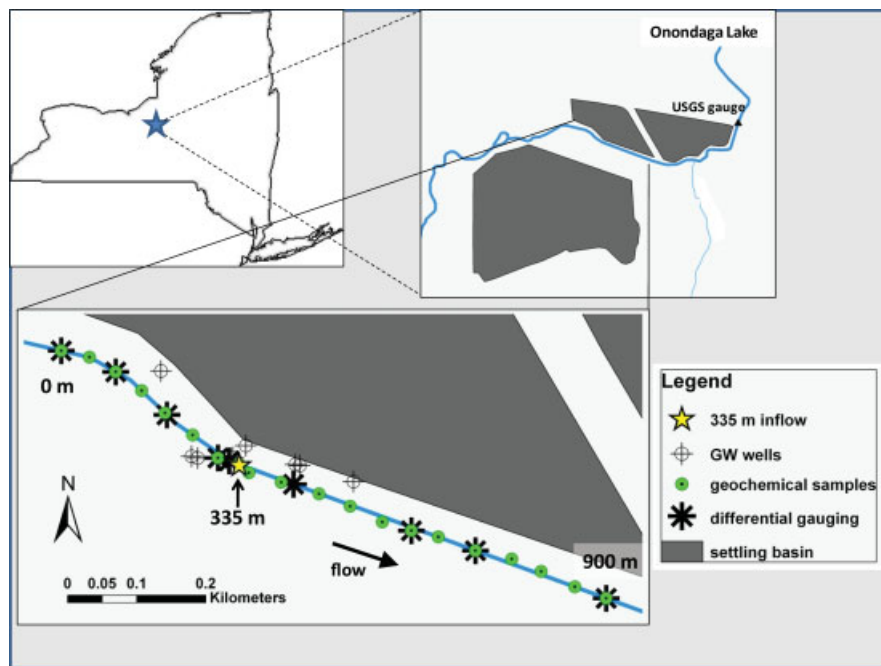
Figure 1. The Ninemile Creek reach and adjacent inorganic salt waste settling basins in Syracuse, New York, USA

tracer breakthrough curves (Kilpatrick and Cobb, 1985; Zellweger, 1994). A combination of the velocity gauging and dilution gauging methods can be used to estimate simultaneous water gains and losses over a stream reach by comparing the tracer mass balance to net stream flow change determined through differential velocity gauging (Harvey and Wagner, 2000; Payn et al., 2009).

Ambient water tracers, such as heat and geochemical constituents, may also be utilized to evaluate groundwater inflows to streams. The ratios between various chemical constituents in solution can be used to determine if the solution is a mixture of two well-defined end-members (Langmuir et al., 1978), which can be incorporated into mixing models to determine groundwater contributions to streams (Robson and Neal, 1990; Land et al., 2000). In particular, dissolved solutes derived from the dissolution of inorganic salts (e.g. Na, Ca, Cl, Br) may be used to source waters influenced by leachate contamination (Christensen et al., 2001; Panno et al., 2006; Whittemore, 2007). Therefore, in cases of groundwater contamination, geochemical mixing models may be particularly useful as the surface water and discharging groundwater likely have distinct chemical signatures resulting in well-defined end members. Quantitative estimates of the magnitude and spatial distribution of groundwater inflows to streams can be made under these circumstances at relatively high resolution when stream waters are well mixed.

Heat has been used formally as a groundwater tracer for over 50 years (Anderson, 2005) and was recognized as a qualitative indicator of groundwater flow to surface waters over 150 years ago (Thoreau, 1854). Many of these methods have been limited by spatially disperse point measurements of temperature, a factor that has recently been resolved by development of fibre-optic DTS technologies for environmental applications.

DTS systems function by initiating a laser pulse down an optical fibre and determining temperature along the fibre by measuring the ratio of temperature-independent Raman backscatter (Stokes) to temperature-dependent backscatter (anti-Stokes) of the laser pulse (Dakin et al., 1985; Grattan and Sun, 2000; Selker et al., 2006b; Tyler et al., 2009). Timing of this backscatter yields a measure of location, which can be resolved to approximately 1-m resolution at the scale of several kilometres. This yields a spatially continuous temperature sensor which can be installed along the stream channel bed to identify groundwater seepage (Selker et al., 2006a; Lowry et al., 2007; Moffett et al., 2008) and provide data for both simple surface water–groundwater mixing models (Selker et al., 2006a) and more complicated total stream heat budget models (Westhoff et al., 2007). We compare emerging DTS technology to differential gauging, dilution gauging and geochemical mixing methods to evaluate the application of DTS to measuring modest (∼5% total stream flow) contaminated groundwater inflow to a large stream in Syracuse, New York, USA. Additionally we explore the sensitivity of groundwater inflow estimates made with DTS data to integration times, time of day when temperature measurements are taken, and the rate of change in stream temperatures over time.

*Study site*

Ninemile Creek is a natural tributary to Onondaga Lake, a 12 km$^2$ water body located adjacent to the northwest corner of Syracuse, New York, USA (Figure 1). The creek drains ∼298 km$^2$ land area, and although the stream is rated second order it has a large average stream discharge of 5·05 m$^3$ s$^{-1}$, which ranges from an average snow melt flow of 9·57 m$^3$ s$^{-1}$ in April to an average base flow of 2·41 m$^3$ s$^{-1}$ in August [US Geologic Survey

(USGS) 04240300 Ninemile Creek at Lakeland, NY; stream flow statistics for 1971–2008]. The lower 5·5 km of the creek are of particular interest because they flow between several large settling basins that were filled with the byproducts of soda ash ($Na_2CO_3$) production from 1944 to the 1980s by Allied Chemical Company, which is now Honeywell Incorporated (Effler and Whitehead, 1996) (Figure 1). Inorganic salts, largely $CaCl_2$, $CaCO_3$, $CaO$ and $NaCl$, dominate the waste material and leach from the settling basins into Ninemile Creek. The creek contributed approximately 1 million metric tons of $Cl^-$ to Onondaga Lake between 1987 and 2000 (Matthews and Effler, 2003).

One likely consequence of salt loading to Ninemile Creek is a degradation of the local recreational fishery. The lower section of the stream has low fish diversity relative to upstream sites, and the dominant fish species are less desirable (Whitesucker, Carp, White Perch) in comparison to upstream sites that are dominated by Brown Trout (Auer *et al.*, 1996). Work has been done by Honeywell Incorporated to remediate some sediments of Ninemile Creek, but there is also interest in identifying the spatial distribution and magnitudes of saline groundwater fluxes to the stream. The 900-m reach of Ninemile Creek selected for this investigation ends approximately 1·5 km upstream of the USGS 04240300 gauge (Figure 1). This reach coincides with a previously identified region of increased stream water salinity (Effler and Whitehead, 1996), which was assumed to reflect the influence of settling basin leachate, although the absolute location and magnitude of groundwater flux had yet to be rigorously quantified. The channelized reach was bound by clays, sands, and coarse cobbles and had extensive macrophyte growth at the time of the experiments.

## METHODS

### Differential and dilution gauging

Differential gauging was performed with a top-setting wading rod equipped with a handheld acoustic doppler velocimeter (SonTek/YSI FlowTracker ADV) that has a velocity range of 0·001–4·0 m s$^{-1}$. This instrument was chosen, in part, because of the integrated software package that allows for several quality control evaluations of each velocity measurement. Additionally, there is a general discharge uncertainty evaluation based on the International Organization for Standardization (ISO) uncertainty calculation or the USGS statistical uncertainty calculation, which are explained in detail in the Flow-Tracker manual (SonTek/YSI, 2009). The ISO method interprets the physical characteristics of each velocity measurement to generate discharge uncertainty estimates, while the USGS statistical method uses adjacent measurements of each estimated variable. As the USGS statistical method always generated a similar or larger uncertainty estimate compared to the ISO method, and has been shown to be more universally reliable (SonTek/YSI,

2009), it was used to more conservatively estimate the uncertainty of each discharge measurement.

All measurements were made during the day on September 9th, 2009 at 6/10 the total stream depth, normal to flow direction, approximately every 100 m except where stream depth was greater than the height of the wading rod (>1·4 m), making measurements unfeasible (Figure 1). Over several transects excessive macrophyte growth was cleared from the streambed to allow a more representative velocity measurement. Repeated measurements were made in sequence at the 900 m location and averaged to determine a 'known' point of discharge for use in the tracer two-component mixing models because the cross-section was uniform, weed-free and much less turbulent than other sections.

Rhodamine water tracer (RWT) dye was used as a conservative tracer to estimate groundwater inflow and discharge by dilution gauging (Kilpatrick and Cobb, 1985). RWT may not behave conservatively in some systems due to sorption (Kasnavia *et al.*, 1999), but this should not significantly affect mixing models generated at plateau concentration where sorption/de-sorption processes should be at steady state. A small bridge focused flow 530 m upstream of the reach head and served as the injection point to ensure the RWT was fully mixed with stream water before entering the experimental reach. Mixing was further enhanced by a multi-drip injection line installed perpendicular to flow. The 20% liquid stock RWT was diluted with stream water to 1640 mg RWT l$^{-1}$ and injected at 500 ml min$^{-1}$ from 11:55 to 13:55 hours on September 9th, 2009. Concentration change through time was monitored with a hand-held fluorometer (YSI 600 OMS) at the 150 m reach location until plateau concentration was reached. After that time, grab samples were collected along the thalweg in several locations and were stored on ice until transport back to the laboratory. There, they were filtered using Whatman GF/F Glass Microfibre Filters and analysed for RWT concentration with an Opti-Sciences GFL-1 fluorometer. Dilution of the injected tracer was used to determine total stream discharge and identify and quantify groundwater influx to the stream reach between sampling locations.

### Ambient tracers

Both the stream and groundwater geochemistry and temperature were used to locate and measure groundwater inputs to the 900-m stream reach. The groundwater temperature was determined with a Traceable Digital Thermometer probe with 0·05-K accuracy. Groundwater was pumped from nine individual wells on both sides of the stream at various depths ranging from 3·0 to 36·6 m (installed by Honeywell Incorporated; Figure 1 and Table I), and from two shallow piezometers (0·45–0·50 m screen depth) installed in a diffuse North-side stream bank seep at approximately the 320-m mark on the experimental reach (Figure 1). Groundwater temperatures were also measured in free-flowing water from the same seep.

Table I. The focused groundwater inflow estimates for the 335-m reach location

| Method | Focused GW inflow ($l\,s^{-1}$) | Estimated error ($\pm l\,s^{-1}$) | Fraction total discharge (%) |
|---|---|---|---|
| *Geochemical mixing models* | | | |
| Cl mixing model | 72.8 | 0.1 | 5.2 |
| Ca mixing model | 68.8 | 0.2 | 4.9 |
| *Dilution gauging* | | | |
| RWT dye dilution | 67.0 | 20 | 4.8 |
| *Differential gauging* | | | |
| ADV flow gauging | *Little net change, noisy data* | | |
| *DTS heat tracing* | | | |
| Mean 24-h | 58.6 | 6 | 4.2 |
| Warmest 2-h (1) | 69.9 | 6 | 5.0 |
| Coldest 2-h (2) | 63.7 | 6 | 4.5 |
| High warming (solar) 2-h (3) | 40.7 | 6 | 2.9 |
| High cooling (night) 2-h (4) | 58.6 | 6 | 4.2 |

Inflow estimates were similar except those generated using temperatures collected during peak solar hours and flow calculations made with the ADV, which were too noisy to identify the small (~5%) inflow. Error was estimated by applying the standard deviations of repeat sample measurement on data specific instruments to the mixing model (Equation 3) over the observed concentration ranges. Numbers following DTS heat tracing methods refer to the time periods indicated in Figures 2B and 5.

Stream temperature data were collected using an Agilent Distributed Temperature Sensor (N4386A) using a 1·5-min sampling interval in dual-ended mode, yielding 3-min integrated 1·5-m spatially distributed temperature estimates for 24 h (17 : 00 September 8th to 17 : 00 September 9th) along the fibre. The instrument collected temperature traces every 10 s on alternating channels along the looped fibre, reversing the directionality of the incident laser to help account for differential signal loss, and these measurements were integrated over 3-min time intervals by the onboard DTS software to yield a single temperature estimate for every 1·5 m of fibre. As suggested by Tyler *et al.* (2009), this integration time was kept short (3 min) to provide flexibility in post-collection data analysis, during which varying longer integration times could be explored. The fibre optics were loosely packed in hydrophobic gel and housed within stainless steel armouring and installed along the reach thalweg at the sediment/water interface. The heavy dense armouring of the cable helped keep the sensor in place along the streambed. Additionally, vegetation was cleared locally in places of thick macrophyte growth and the cable was anchored with flat river stones in regions of high velocity.

An initial 34 m of fibre was coiled in a cooler kept packed full with ice and interstitial water for calibration purposes (Tyler *et al.*, 2009). The calibration bath temperature was independently monitored with a Thermochron iButton with 0·5-K accuracy and 0·0625-K precision. In double-ended mode the tandem fibres in the cable are fused at one end to allow a single pulse from the instrument to measure temperature twice at

every reach location, including the ice bath, aiding in calibration of the data. A slight temperature offset and systematic drift of the instrument over the 24 h period were identified by comparing the iButton temperature record to the temperatures recorded at the coiled fibres in the bath. The entire data set was adjusted in MATLAB™ by removing the systematic drift and offset through time from the entire stream temperature record. The cable was geo-referenced along the reach by linearly modifying (stretching or compressing) the distance measured by the DTS unit using the return speed of the laser to known points on the cable every 50 m. Known points were identified by exposing the submerged cable to warmer air at 50 m increment thalwag points determined with measuring tape, and finding those warm points within the temperature trace. This adjustment was typically on the order of a few metres or less, and differences between the 'actual' and DTS distance estimates were likely due to the loose packing of the fibres within the outer cable, and slight meandering of the cable over the streambed.

The 24-h mean stream temperature was calculated every 1·5 m along the cable to spatially identify areas of relatively low temperature, which indicates the influence of a constant, low temperature groundwater source (Constantz, 1998). In the late summer, surface waters are warmer than the regional groundwater (~12 °C), and therefore areas of focused groundwater inputs should be consistently colder than other stream segments and the cooling effect should persist a measurable distance downstream. In contrast, hyporheic exchange can buffer diurnal temperature changes by moderating both stream warming and cooling, which can be distinguished from constant cold groundwater inflows (Loheide and Gorelick, 2006). Bed conduction may affect equilibrium stream temperatures due to cold groundwater at depth, but it was assumed that the only process of sufficient magnitude to decrease mixed stream temperature in stepwise fashion in this large stream was focused groundwater inflows. The 24-h mean temperature distinguishes consistently cold areas from the variable heating and cooling of the channel resulting from sensible, latent, and short/long wave energy fluxes over the diurnal period, influences which can have great effect on shorter duration temperature integrations. Assuming groundwater inflow is consistent over the 24-h period a simple quantitative estimate of groundwater flux to the stream can be made using the change in mixed stream temperature from above a point where stream water temperature decreases to below that point using a two-component mixing model derived from the following relationships:

$$Q_i T_i + Q_{gw} T_{gw} = Q_o T_o \qquad (1)$$

$$Q_i + Q_{gw} = Q_o \qquad (2)$$

where $Q$ is discharge, $T$ is temperature, and subscripts $i$, $o$ and $gw$ refer to the stream water into the section, out of the section and groundwater inflow over the section, respectively. These equations can be combined to solve
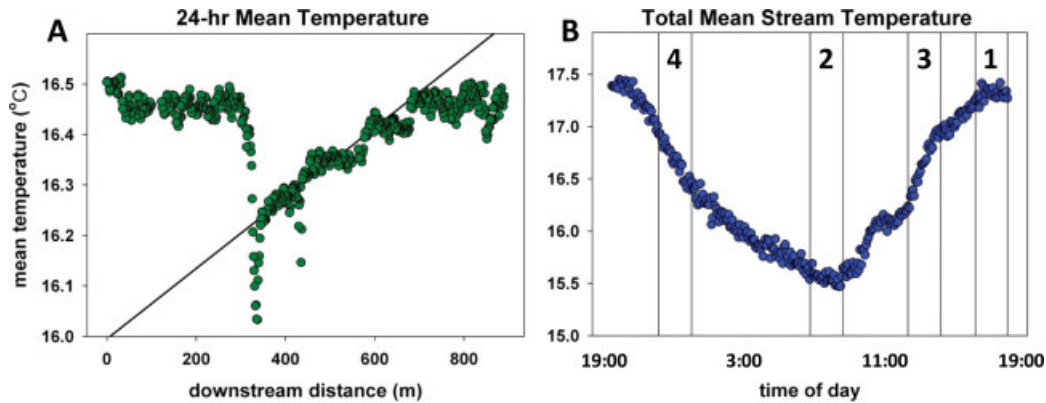
Figure 2. Panel A depicts the 24-h mean temperature with distance, clearly showing the focused groundwater input at 335 m, which lowered stream temperature by 0·26 °C, generating a focused groundwater inflow estimate of 58·6 ± 6 l s$^{-1}$. A curve fit to the return of mixed stream water to ambient temperature was used to both identify the unmixed groundwater signals and the duration of downstream affect, which was estimated to be approximately 400 m. Panel B shows total stream temperature as a function of time. High rates of change were observed in late evening (4) and mid-afternoon (3). The groundwater inflow estimate calculated during these 2-h time periods was poorest for (3) when solar input was highest, while groundwater inflow determined when stream temperature was relatively stable (1, 2) generated estimates in closest agreement with other methods

for the groundwater discharge over the cold section as (Kobayashi, 1985):

$$Q_{gw} = Q_i \left[ \frac{T_o - T_i}{T_{gw} - T_o} \right] \qquad (3)$$

We determined $Q_o$ with repeat FlowTracker measurement within an 'ideal' cross-section at the end of the reach with low velocity, no macrophyte growth and uniform bed morphology, and $Q_i$ was derived from this using the model with the observed change in temperature. $T_i$ and $T_o$ were taken as the 50 m mean temperature bracketing a focused point of stream cooling, or the mean temperature over a distance of 50 m above and 50 m below such a point, respectively.

If the cable passes directly over an area of groundwater inflow at the streambed interface, the groundwater at that point is likely not completely mixed with the water column. The result is 'anomalous' cold temperature measurements that may result in local overestimation of groundwater flux. Such cold points were identified by fitting a line to the mixed stream temperature data below the cold water input to identify outliers (Figure 2), and these points were removed from the 50 m downstream mean. In addition to $Q_{gw}$ determined from the 24-h mean temperature record, an estimate of $Q_{gw}$ was made for every individual time-step of the double-ended measurement (i.e. every 3·0-min integration) and for several different 2-h time intervals over the 24-h record. These varied time interval estimates were used to evaluate method sensitivity to system noise, temporally varying differences between the stream and groundwater temperature, and rates of overall stream temperature change with time.

In-channel stream water chemistry samples were taken along the thalweg at 50 m increments along the 900 m reach, and groundwater samples were collected from the same well locations where temperature was measured (Figure 1). Samples were kept cooled (temperature <4 °C) and filtered upon return to the lab where they were analysed for $Ca^{2+}$, $Na^+$ and $Cl^-$ using Ion

Chromatography (Dionex ICS-2000). These three ions are known to be present naturally in regional surface waters and concentrated in local groundwater due to settling basin leachate. Bi-variate ratio–ratio plots of stream water Cl : Na and Ca : Na were used to evaluate whether stream water was a simple mixture of two consistent and distinct end members. A linear trend on a plot of two ratios with common denominators indicates two end-member mixing (Langmuir et al., 1978). The groundwater concentrations from various sources (e.g. wells at various depths/locations and piezometers) were also depicted on this plot to help identify the appropriate end member for the mass balance mixing analysis. The magnitude of $Q_{gw}$ for focused inflows was determined using mixing models in the same manner as shown in Equation 3, with $T$ replaced by either $[Ca^{2+}]$ or $[Cl^-]$. Transport of $Ca^{2+}$ and $Cl^-$ was assumed to be conservative on the timescales of local surface water–groundwater exchange in this system.

We determined the expected error range for each groundwater inflow estimate generated using heat, dye and geochemical methods from the precision of the temperature, Rhodamine WT and solute observations used in the mixing models, respectively. We estimated the precision of temperature, dye and solute observations using the standard deviation of repeat measurements of each parameter. Assuming the groundwater end-member is known, the absolute error of the groundwater inflow estimate is a function of both the data precision and the relative difference between the surface water and groundwater temperatures or concentrations. Because the groundwater inflow estimates are generated from the difference between measurements that bracket the inflow, the error of these respective measurements must be taken into account when using the mixing model (Equation 3). The inflow must modify mixed stream temperature or concentration by more than twice the data precision for such a change to be considered significantly different from zero. We approximated the range of error of each individual groundwater inflow estimate by modifying the
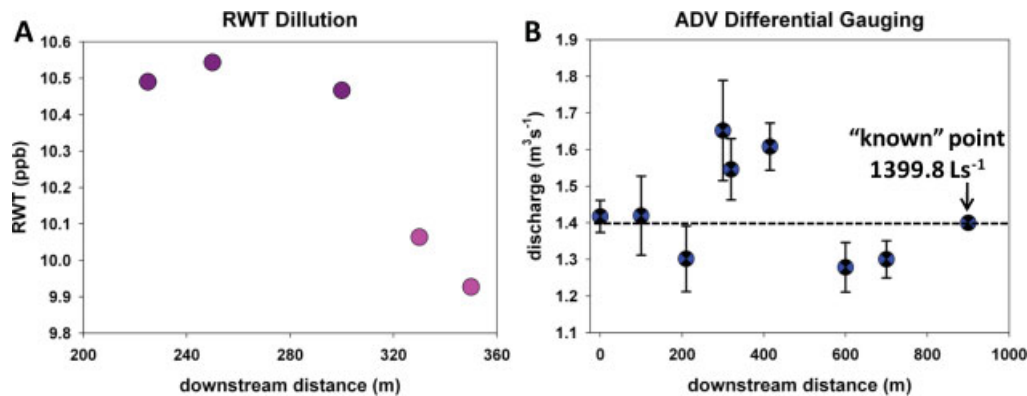
Figure 3. Plot A shows the dilution of the RWT tracer over the focused input that produced a groundwater inflow estimate of $67 \cdot 0 \pm 20$ l s$^{-1}$. Plot B displays estimates of total stream discharge made with the ADV, which were highly variable with a standard deviation of 130 l s$^{-1}$, but showed no net change over the reach. Error estimates generated using the ADV software and USGS statistical uncertainty method underestimated true error, which is larger than the groundwater inflow magnitude in question. Identical repeat measurement at the 900 m cross section under ideal conditions were used as the starting point for all mixing models (1399·8 l s$^{-1}$), and this value was corroborated by RWT dilution

upstream and downstream temperature or concentration observations used in the heat or geochemical mixing models by the estimated precision of the values. The error for each method also theoretically corresponds to the smallest measureable groundwater inflow using each method. These numbers are specific to this experiment as the estimates of error (or sensitivity) are reflective of both intrinsic instrument error, and the range and difference in observed surface water–groundwater temperatures or chemical concentrations at this site at the time of the experiment. In addition, as this error method is based only on instrument sensitivity, other possible errors based on factors such as mixing are not included (Schmadel *et al.*, 2010).

## RESULTS

### Differential and dilution gauging

Flow at the USGS gauge (04240300) downstream of the study site indicated net discharge from lower Ninemile Creek remained constant for the 24-h study period. Repeat discharge estimates generated at the 900-m 'ideal' cross section with the acoustic Doppler velocimeter (ADV) were identical (1399·8 l s$^{-1}$) providing a known point for the mixing model analysis. Stream discharge estimates made at eight other locations along the reach with the ADV were highly variable in magnitude (Figure 3) with a standard deviation of 130 l s$^{-1}$, while mean velocities for the cross sections ranged from 0·08 to 0·53 m s$^{-1}$. Variations in discharge displayed no clear pattern based on physical processes, and there was virtually no net change in discharge from the head to end of the reach (Figure 3). There was an apparent increase in stream discharge around the 335 m reach location, but this is followed by apparent loss to the 600 m location and a return to the upper reach boundary discharge by the 900 m location. This variability was significant according to the USGS statistical uncertainty analysis, which determined a mean flow uncertainty of 5·6%. The conditions for making velocity measurements were poor in many locations due to high turbulence, high and variable velocity, variable bedform, depth and excessive macrophyte growth. This resulted in several measurements with high signal to noise ratio, high angle to flow, and although at least 14 measurements were taken for each cross section, representative sections of many cross sections exceeded 10% of overall flow.

The RWT injection identified a groundwater inflow around the 335-m location, as stream concentrations dropped from an average plateau of 10·5 ppb RWT above to 10·0 ppb RWT below the inflow (Figure 3). The standard deviation of repeated RWT concentration measurements within this concentration range was determined to be 0·07 ppb. The relative precision of the RWT concentration measurements yielded the largest estimated error range (lowest sensitivity) for any of the mixing model methods of $\pm 20$ l s$^{-1}$. The injection was also used to estimate total stream discharge below the input based on dilution of the tracer, which was 1360·0 $\pm$ 10 l s$^{-1}$ and comparable to the repeat differential gauging measurement of 1399·8 l s$^{-1}$.

### Ambient tracers

A plot of stream temperature against time and distance clearly showed a short stretch of thalweg from 325 to 340 m that was consistently colder than the rest of the reach (Figure 4). Also evident was the persistent cooling effect of this input on downstream water temperatures for several hundred metres. The exact location of this colder zone was determined by exposing the submerged cable to warmer air at the location of the cold signal in the temperature trace, analogous to how the cable was geo-referenced. There were two much smaller areas of persistently colder stream temperatures at approximately 112 and 430 m, but these had no measurable downstream temperature influence. Further inspection of the field site revealed that the 430-m location was likely a very small localized groundwater spring, but the 112-m 'cold' spot may have been an artifact of a damaged fibre as no cold input was found there using an independent temperature probe.
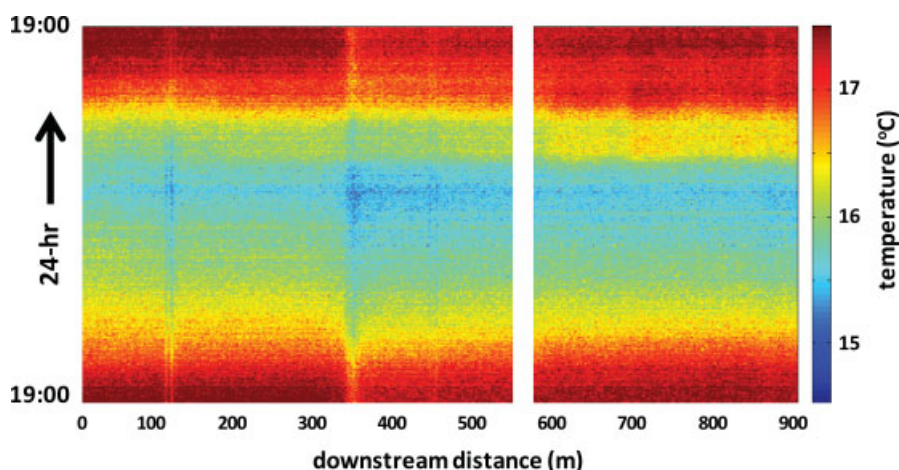
Figure 4. Stream temperature at 1·5 m spatial resolution integrated over 3·0 min sampling intervals over 24 h starting at 19 : 00 on September 8th, 2009. The strong diurnal signal was consistently cooled around the 335 m reach location with persistent downstream affect. A splice in the fibre generated erroneous data at 580 m and was removed, and the 'cold' spot at 112 m was likely an artifact
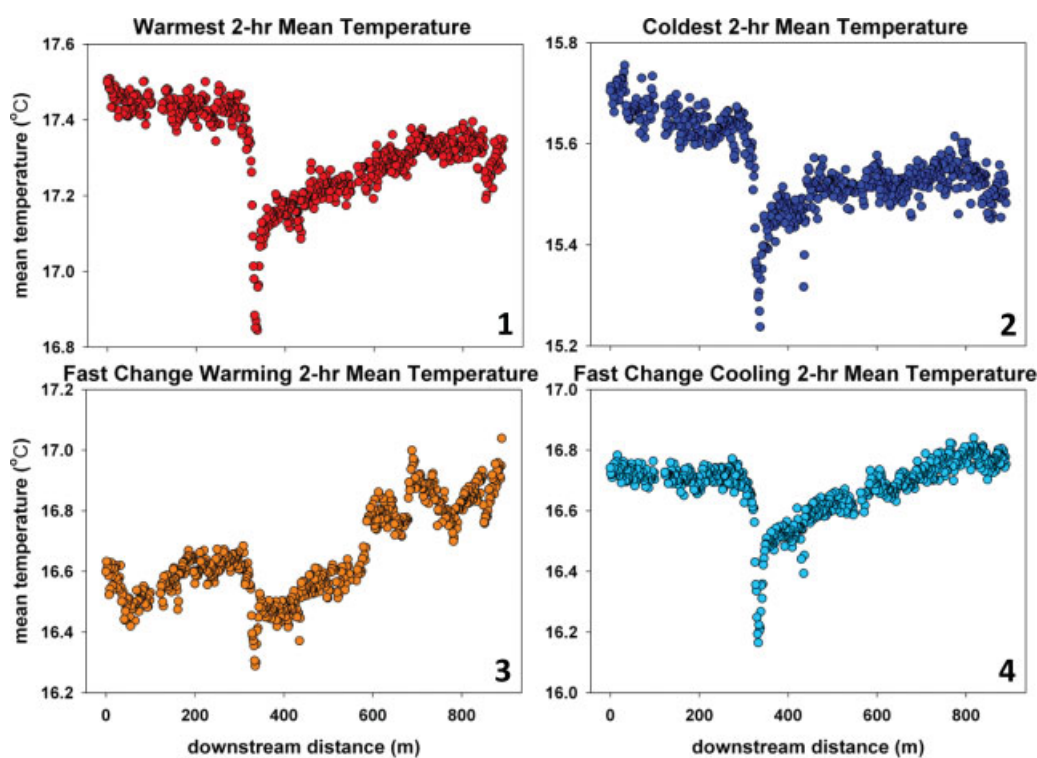


Figure 5. Various 2-h mean stream temperatures with reach distance that all clearly show the influence of groundwater centred on the 335 m location, with the exception of plot 3, which was generated from the time of peak solar input and high temperature change. Plots 1 and 2 depict when stream temperatures were at their warmest and coldest respectively, and generated inflow estimates most similar to other methods ($69.9 \pm 6$ l s$^{-1}$, $63.7 \pm 6$ l s$^{-1}$) as overall stream temperature was most stable (Figure 2). Differential heating of the stream depicted in plot 3 yielded the poorest inflow estimate ($40.7 \pm 6$ l s$^{-1}$) while inflow calculated when the stream was cooling rapidly yielded the same value as the 24-h mean ($58.6 \pm 6$ l s$^{-1}$)

When the 24-h mean temperatures from the DTS dataset were plotted with distance, the inflow around 335 m was even more apparent (Figure 2). The mean temperature for 50 m above the input was 0·24 °C higher compared to the 50 m mean from directly below the input. This change is much larger than the estimated precision of the measurements, which were ±0·01 °C, based on the standard deviation of the 2-h mean temperature over a 30-m distance for the ice bath calibration coil. The standard deviation of the 2-h mean ice bath temperatures generated an error estimate of ±6 l s$^{-1}$

for this temperature range. This value corresponds to a conservative estimate of error for the 24-h mean temperature which likely had higher precision, but this could not be directly determined by repeat measurement as there was only one 24-h period recorded. The 24-h mean stream temperature was used to quantify the groundwater inflow at $58.6 \pm 6$ l s$^{-1}$, which was similar to that determined with 2-h means taken during the coldest ($63.7 \pm 6$ l s$^{-1}$), warmest ($69.9 \pm 6$ l s$^{-1}$) and fastest cooling ($58.6 \pm 6$ l s$^{-1}$) portions of the diurnal temperature cycle (Figure 5, Table I). The inflow calculated
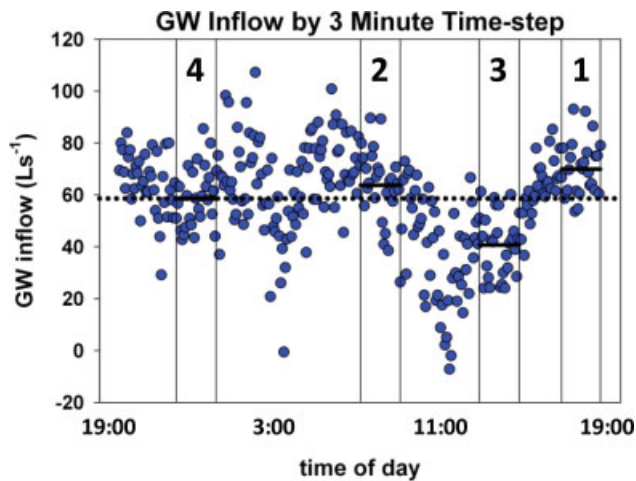
Figure 6. The variable groundwater inflow estimates made for each 3 min time-step of the double-ended DTS measurement with the 24-h mean of $58 \cdot 6 \pm 6$ $1$ $s^{-1}$ as the dotted line. This mean is decreased by data collected during the daylight hours of peak solar radiation. Times of slow and fast overall stream temperature change are shown (Figure 2B) with solid lines depicting their respective means



Figure 8. Stream water Cl to Na and Ca to Na ratios fall on a straight line indicating mixing of two distinct groundwater end members, with a distinct jump at the 335 m focused input. The shallow bank piezometers generally plot along this line, along with some deeper groundwater wells. The groundwater wells at various depths and locations also display another mixing pattern, likely between leachate and deep bedrock brine

as the stream was warming at the highest overall rate was found to be significantly less than these values ($40 \cdot 7 \pm 6$ $1$ $s^{-1}$). Inflow estimates made with the original 3-min time-step were variable with a larger range error of $\pm 31$ $1$ $s^{-1}$ (Figure 6), which generally encompassed the inflow values determined using the 24- and 2-h means, with the consistent exception of values during the mid-day.

Stream chemistry changed abruptly around 335 m, and after initial mixing, a stable chemical composition was sustained for the remainder of the reach (Figure 7). Stream samples from 50 m above the 335 m input were compared to the $400-900$ m reach chemistry and showed a total increase in $Cl^-$ of $324 \cdot 3 \pm 0 \cdot 1$ ppm, and of $Ca^{2+}$ of $95 \cdot 3 \pm 0 \cdot 2$ ppm, both of which represented similar proportional increases from their respective upstream values. The ratio–ratio plot of $Cl : Na$ and $Ca : Na$ in mixed stream water yielded a linear relationship as the stream water evolved towards groundwater concentrations with

downstream transport. This confirmed the use of two end-member geochemical mixing models of $Cl^-$ and $Ca^{2+}$ using stream and groundwater concentrations (Figure 8). Both the $Cl^-$ and $Ca^{2+}$ mixing models produced similar precise focused groundwater inflow estimates around the 335 m reach location of $72 \cdot 8 \pm 0 \cdot 1$ $1$ $s^{-1}$ and $68 \cdot 8 \pm 0 \cdot 2$ $1$ $s^{-1}$, respectively. In addition, the chemical mixing models indicated there was a net total diffuse groundwater inflow of $\sim 12$ $1$ $s^{-1}$ over the 75 m stream reach leading up to the more focused input which was not apparent from the temperature and dye data.

## DISCUSSION

### Spatial distribution of groundwater inflow

The 900-m experimental reach had a focused groundwater inflow centred at the 335 m reach location, as was identified most clearly from the ambient heat and geochemical tracing. Heat tracing, in particular, provided the highest spatial resolution, allowing the inflow to be
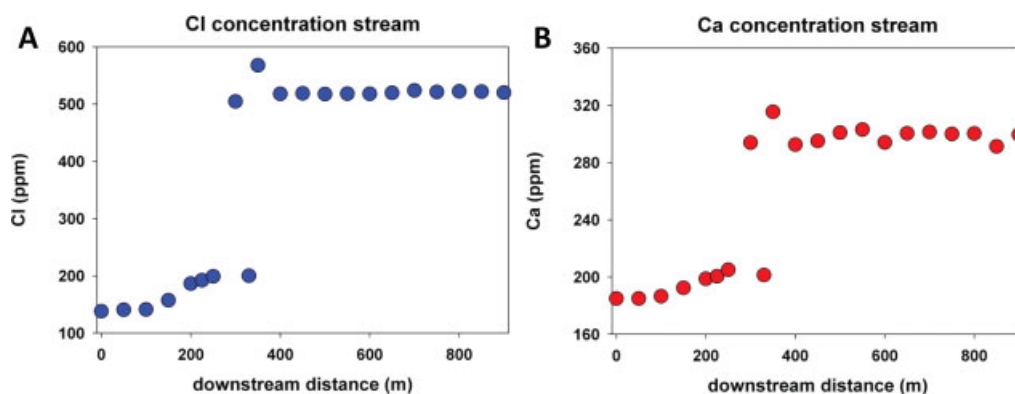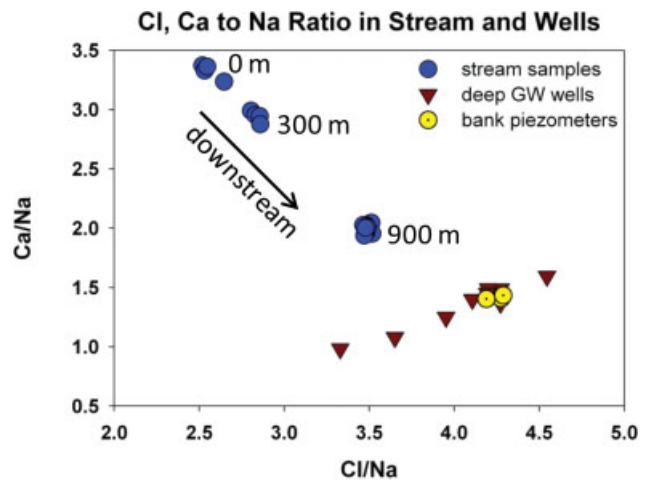


Figure 7. Plots A (Cl) and B (Ca) both show a sharp increase in concentration around the 335 m input with some mixing noise downstream of the input. This shift in concentration was used to calculate a focused groundwater inflow of $72 \cdot 8 \pm 0 \cdot 1$ $1$ $s^{-1}$ for Cl and $68 \cdot 8 \pm 0 \cdot 2$ $1$ $s^{-1}$ for Ca. The slight increase in concentrations for $\sim 75$ m leading up to the focused input indicated diffuse groundwater inflow of approximately 12 $1$ $s^{-1}$ not captured by other methods

pinpointed at the 1·5-m scale. The groundwater input had a persistent cooling effect on stream temperatures until the 730-m location. This distance was calculated by fitting a line to the linear re-warming of stream temperature and determining where this line reached the mean observed upstream of the input (16·5 °C). A two sample $t$-test ($p = 0.69$) indicated that the mean stream temperature was not statistically different between the region upstream of the input and stream temperatures after 730 m, but did vary significantly before this point downstream of the input ($p < 0.001$). The fitted line was also used to identify outliers from the mixed stream temperature (Selker et al., 2006a), which were very cold areas recorded as the cable passed directly over springs through the streambed. These values were generally localized to the 325–340 m location and were not included in the mixing model as they did not reflect mixed stream water temperatures. This result illustrates the strength of the DTS method as a reconnaissance tool for precisely locating groundwater inflows. Cold areas can also result from stratification of stream waters (Neilson et al., 2010), especially in deep pools, but the flow velocities, mixing and morphology of this reach indicated stratification was likely not an important factor.

The cold section identified by the DTS at 335 m coincided with a sharp change in stream water chemistry longitudinally along the creek. The chemistry data are more sensitive to small groundwater inputs (minimum groundwater input estimate precision of $\sim \pm 0.2 \, l \, s^{-1}$) than temperature at this site (minimum groundwater input estimate precision of $\sim \pm 6 \, l \, s^{-1}$), given the high precision of the solute concentration data and very large geochemical gradient between stream water and groundwater, and therefore can allow the identification of diffuse inputs. The geochemical method identified diffuse inputs over the $\sim 75$ m above the focused input, which was not detected with the heat tracing (Figure 7). Despite this advantage of geochemical mixing at this site, large geochemical gradients are unique to this location and the grab samples are spatially limited compared with the continuous DTS sensor. Further, the instantaneous nature of point grab-sampling renders them susceptible to mixing issues which can be influential in a large, fast flowing stream and may explain the noisy data directly below the 335 m input. In contrast, the DTS data are integrated through space and time which reduce mixing noise. Similar to previous research (e.g. Selker et al., 2006a; Lowry et al., 2007; Moffett et al., 2008) we found that installation of the cable directly on the streambed over springs can lead to measurement of groundwater inflow unmixed with surface water. As discussed, this may actually be viewed as a benefit in terms of identifying the exact locations of groundwater inflows, and these points can be easily isolated from the mixed stream temperature by fitting a curve to the mixed data, and can therefore be excluded from mixing model analysis.

Dye tracing identified an apparent focused groundwater inflow around 335 m which agreed with the other methods as the mixed stream RWT concentration dropped by a mean of 0·5 ppb. Introduced tracers may be problematic because it can be difficult to determine when the stream is truly at a plateau concentration, particularly if flow conditions are transient. This limitation may have affected data collected further downstream within the experimental reach in this study and, consequently, that data were not included in the RWT groundwater discharge calculations. As with instantaneous chemical samples, lack of groundwater mixing may compromise RWT data as was shown by Schmadel et al. (2010) who found that mixing uncertainty represented the majority of the $\pm 8.4\%$ estimated error they rigorously determined when using the dilution gauging method. Without the supporting heat and chemical data it might be difficult to definitively attribute a 0·5 ppb change in RWT concentration to the physical process of groundwater gain.

Non-ideal field conditions such as large depth and turbulence, variable velocity and bedform, and an abundance of macrophyte growth adversely affected differential gauging measurements. The integrated software of the FlowTracker ADV helped to identify some of these possible sources of error, but the general discharge uncertainty measurements generated by both the USGS statistical method and the ISO method appear to have underestimated the true uncertainty. This is consistent with previous work that found current meters performed poorer than their respective manufacturers published accuracy limits (Fulford, 2001). Perhaps a finer measurement spacing and further clearing of macrophyte growth would have provided more accurate discharge estimates, but both of these activities can be treacherous within a deep, fast flowing large stream. Our results were similar to that found by Soupir et al. (2009) who compared various gauging techniques to a control discharge in two small steams. The two ADV devices they tested (which did not include the FlowTracker ADV) had median percent relative error that ranged from 57·7 to 122·2%. Other instruments used for measuring velocity (four current meters) generally had better agreement with the control discharge, but none had a median percent relative error less than 24·0%, which is far greater than the 5% increase in flow found at Ninemile Creek. Interestingly, one of the worst performing methods tested by Soupir et al. in two small streams was dilution gauging using RWT, which had a median percent relative error of 58·7%. They attributed this error in part to inadequate mixing across the reach length, although the method for determining the correct length prescribed by Kilpatrick and Cobb (1985) was followed.

### Comparison of groundwater inflow estimates

All of the methods discussed above, with the exception of differential gauging, provided similar estimates of focused groundwater inflow centred around the 335-m reach location with a mean of 66·8 $l \, s^{-1}$ with the geochemical methods providing the highest precision (Table I). The focused nature of this inflow may result from the re-routing of Ninemile Creek during settling

bed construction from its natural channel into clay and fill deposits (unpublished data provided by O'Brien and Gere, 2011), forcing down-valley groundwater flow to the surface. Some dense clay material is evident along the banks and in the well logs from this area. Although in an absolute sense this inflow is large, it only represents a 4·8% increase in total stream discharge (Table I), which is modest compared to previous studies using DTS in smaller streams (Selker *et al.*, 2006b). Differential gauging indicated little net change in stream flow over the reach, and error estimates made with the ADV software likely underestimated true error and exceeded the inflow in question. This is consistent with previous work which found differential gauging with the same ADV unit did not capture gains from groundwater springs identified by DTS when the magnitude of these gains was within the ADV measurement accuracy (Lowry *et al.*, 2007).

The 24-h mean heat tracing estimate of $58·6 \pm 6 \, 1 \, s^{-1}$ was determined using Equation 3 and the change in mean mixed stream temperature of $0·26 \, °C$ between the 200–250 and 350–400 m reach lengths. Although the 24-h mean is an effective method for identifying groundwater inflow, it may not be the most appropriate for determination of flow magnitude. Estimates of groundwater inflow based on shorter time scales (i.e. 2 h) when total stream temperature was relatively steady produced results more comparable to the other methods, and this sensitivity effect is discussed in the following section. For this study, groundwater temperature used for the mixing model was determined from shallow piezometers, but in systems such as bedrock lined reaches installation of wells may not be feasible. In these settings groundwater temperature may be determined from the mixed stream temperature when it is found to be consistent across a region of known groundwater inflow, assuming the stream water reaches groundwater temperature at some point over the diurnal cycle (Selker *et al.*, 2006b).

The mixed stream chemistry had a large shift in the ion ratios around the 335 m location, and evolution of stream water towards groundwater concentrations above the 335 m inflow indicated diffuse groundwater inflow (Figure 8). An increase in both the $Cl^-$ and $Ca^+$ concentration at the focused input yielded similar focused inflow estimates of $72·8 \pm 0·1$ and $68·8 \pm 0·2 \, 1 \, s^{-1}$, which are somewhat larger and outside of the error bounds of the 24-h mean temperature estimate. The ratio–ratio plot of groundwater from wells at various depths adjacent to the stream produced a different linear mixing line than that observed for the stream (Figure 8), likely the result of mixing between leachate influenced groundwater and deep basin brines. Given the large variability of the groundwater composition (e.g. Ca : Na and Cl : Na ratios) and the groundwater $Ca^{2+}$ and $Cl^-$ concentrations, the groundwater end-member chosen for this analysis was that collected from the shallow piezometers in the stream bank seep, as these samples were in close physical proximity to the focused streambed input and generally fell along the stream water mixing line (Figure 8 and Table II).

Table II. Chemical constituents of interest in the local groundwater in wells at varying depths and distance from the 335 m focused inflow

| Well number | Cl (ppm) | Ca (ppm) | Na (ppm) |
|---|---|---|---|
| *Shallow bank samples* | | | |
| Piezometer 1 (0·45–0·50 m) | 6,295.0 | 2,071.0 | 1,472.0 |
| Piezometer 2 (0·45–0·50 m) | 6,718.0 | 2,245.0 | 1,567.0 |
| seep (surface) | 6,278.0 | 2,103.0 | 1,498.0 |
| *Deeper groundwater samples* | | | |
| WB05M (16·2–19·2 m) | 12,006.0 | 3,544.0 | 3,288.0 |
| WB05D (33·5–36·6 m) | 70,036.0 | 20,668.0 | 21,032.0 |
| MW70S (4·6–7·6 m) | 9,074.0 | 3,183.0 | 1,996.0 |
| MW70D (16·2–19·2 m) | 45,295.0 | 15,766.0 | 10,599.0 |
| MW59S (3·0–6·1 m) | 11,275.0 | 3,605.0 | 2,639.0 |
| 85/S (4·9–7·9 m) | 6,829.0 | 2,157.0 | 1,728.0 |
| 85/D (20·6–23·6 m) | 53,243.0 | 18,876.0 | 12,677.0 |
| 85/I (13·4–16·5 m) | 44,732.0 | 15,468.0 | 10,665.0 |
| 84/D (16·6–19·7 m) | 51,927.0 | 17,692.0 | 12,644.0 |

The mean of the similar shallow bank samples was used for the two-end member mixing model with stream water to determine groundwater inflow. Many of the deeper groundwater wells, especially the 84/85 series from the south side of the stream, had similar chemical ratios as the shallow samples but were more concentrated and would have provided an underestimate of groundwater discharge if they were used in the mixing models.

In point-source contaminated streams, such as Ninemile Creek, with two well-defined end-members, geochemical mixing models are an effective tool for estimating groundwater inflow because chemical gradients between the surface water and groundwater are large and data precision is high. Although even in these settings the geochemical method is limited by the need to identify the 'true' groundwater end-member, and whether this end-member is constant in space and time (Kalbus *et al.*, 2006). Figure 8 underscores this concern, as many of the deeper groundwater wells had similar chemical ratios to the piezometers and also fell along the stream water mixing line, yet their concentrations were highly variable (Table II), likely resulting from differential dilution from recharge. If the more concentrated groundwater end-members from the deep wells were used in the mixing models, the focused groundwater input to the creek would have been greatly under-estimated. Therefore, identifying changes in mixed stream chemistry and actually quantifying rates of groundwater inflow are different, the latter being dependent on identifying a correct groundwater end-member that is constant in space. Large errors outside of those derived from concentration measurement precision may be incorporated into groundwater inflow estimates if the groundwater end-member is variable, a concern which is evident from the groundwater chemistry at this site. This, combined with the potential problems with using introduced tracers such as RWT as discussed above (e.g. sorption, mixing, plateau), may render heat tracing more reliable in stream systems where end-members are difficult to characterize.

The heat, chemistry and dye mixing models all resulted in similar groundwater inflow estimates that were approximately 5% of total overall stream flow, although groundwater inflow estimated from dilution of RWT was the

least precise. This modest input is likely too small to be captured with differential gauging, even in ideal conditions. In large streams such as Ninemile Creek, a 5% inflow of contaminated groundwater can represent a significant mass input. For example, if this one focused inflow has been relatively constant in magnitude and concentration through time, it could have contributed over 13% of the approximately 1 million metric tons of $Cl^-$ estimated to have entered Onondaga Lake from lower Ninemile Creek over the years 1987–2000 (Matthews and Effler, 2003).

*Sensitivity of heat tracing inflow estimates to integration time and time of day*

Once the fibre-optic cables are installed in a stream, DTS can produce extensive data sets and often the challenge is to then determining the correct system parameters to best characterize the stream process in question. DTS precision is proportional to the square root of time, increasing with the number of photons collected, which better defines the Stokes to anti-Stokes backscatter ratio and subsequently improve temperature measurements (Tyler *et al.*, 2009). Longer integration times, while more precise, may mask the complexity of stream processes, such as propagation of the diurnal signal through the bed (Hatch *et al.*, 2006; Keery *et al.*, 2007). Previous work by Selker *et al.* (2006a) in a very small stream ($1–2\,l\,s^{-1}$) quantified groundwater inputs that made up a large fraction of total flow using the mixing model method and short DTS integration times. For our larger system, with comparatively smaller groundwater inputs (5%), we found that when the focused groundwater inflow was calculated using the specified fundamental 3-min time-step the noisier data resulted in an expected error range of $\pm31\,l\,s^{-1}$ in contrast to the $\pm6\,l\,s^{-1}$ estimated for the 2-h integration times (Figure 6). This variability is generally clustered around the mean inflow determined through dilution gauging and geochemical tracing ($69.5\,l\,s^{-1}$), with systematic negative deviation from this mean outside of the estimated error range during the daylight hours when solar radiation inputs were large. Many estimates of groundwater influx made during the middle of the day were extremely small or even negative, indicating the stream was warming faster downstream of the 335 m inflow location than upstream. Interestingly, the standard deviation of the 3-min time-step inflow estimates was not significantly larger during times when stream temperature was changing rapidly, further indicating longer integration times are necessary to reduce systematic noise and to more accurately determine modest groundwater inflow even when stream temperatures are relativity stable.

The rate of change in stream temperatures and differential heating of the channel varies over the diurnal cycle due to a combination of environmental factors that affect how the stream gains, retains and loses energy (Figure 2). Estimates of groundwater inflow may be adversely affected, as heat tracing may no longer be

initially 'conservative'. This concern is particularly pronounced during the hours of peak solar radiation, when the stream is heated differentially due to depth, shading, streambed colour, water velocity, turbidity and macrophyte growth. Recent research has shown that DTS deployments along the streambed are sensitive to heat conduction from sediments in contact with DTS cable, particularly in shallow, clear streams, and this process may impair measurement of bulk stream water temperature (Neilson *et al.*, 2010). Therefore, in streams where the sediments are directly warmed by solar radiation, a DTS installation along the streambed interface may be influenced by sediments that are warmer than the mixed water column. In addition, Neilson *et al.* (2010) found that the cable itself may be directly warmed by short wave radiation under certain conditions. The 24-h mean temperature incorporates time intervals when steam temperatures change quickly and incoming solar radiation is at a peak, and therefore may incorporate avoidable error in the groundwater inflow estimate. In the case of this study, the effect was to lower the overall inflow estimate by including anomalously low estimates of inflow determined during the hours of peak solar radiation.

We calculated the 2-h mean DTS temperatures with distance as a method to dampen system noise found in the 3-min measurements by providing a longer integration time, but still allow for greater focus on a specific time of day and rate of change in stream temperature over time (Figure 2B). Groundwater inflow estimates generated using the 2-h means at the coldest ($63.7\,l\,s^{-1}$) and warmest ($69.9\,l\,s^{-1}$) sections of the diurnal temperature cycle were in best agreement with those made using the chemical and dye methods (Figure 5). These times corresponded with the slowest rates of overall stream temperature change with time and when solar input to the stream was low. Conversely, groundwater inflow estimates made over the 2-h interval when stream temperature had the highest and most uneven rate of change during peak solar radiation input provided the least comparable estimate to the other methods ($40.7\pm6\,l\,s^{-1}$). During this time the downstream temperature was warmer and more variable than upstream, likely due to direct differential heating of the bed in shallow, slow flowing areas. This incorporated error into the inflow calculation in addition to that determined through the sensor precision error analysis discussed above. In that case the bed surface would not be in equilibrium with the mixed water column above, and would influence temperature measurements made along the adjacent DTS cable. These influences were so pronounced that the 2-h afternoon trace (Figure 5, panel 3) shows temperature step changes of similar magnitude to the true groundwater inflow, indicating physical hydrologic gains that do not actually exist. The estimate of groundwater inflow made when the stream was cooling quickly during late evening did not exhibit nearly as large a deviation from the other methods as the mid-day estimate, producing the same result as that made using

the 24-h mean ($58.6 \pm 6$ l s$^{-1}$). This indicates differential heating and possible direct warming of the sediments with conduction to the cable are the major sources of error rather than the stream simply not being at some relative temperature equilibrium.

These results suggest that although the 24-h mean stream temperature may be an effective tool to identify groundwater inflows to streams, it can be influenced by differential heating and potentially bed conduction during peak solar radiation. Estimates of groundwater inflow integrated over several hours when the stream has the slowest rate of overall temperature change provided results most consistent with the chemical and dilution gauging methods, and had much greater precision compared to the 3-min integrated estimates. As temperature records can be averaged over time with relative ease during post processing, it may be best to record data at a relatively fine time step, such as 3 min in this case, and increase those integration times after a preliminary review of the data to best characterize the process in question. Regardless, data collected during the hours of peak solar radiation should not be used to quantify groundwater inflow.

## CONCLUSIONS

The longitudinal stream 24-h mean temperature, Cl$^-$ and Ca$^{2+}$ chemistry, and RWT dilution methods all identified both the location and magnitude of a focused inflow of saline groundwater to Ninemile Creek, though their spatial resolution and limitations differed. The absolute inflow magnitude estimates were all quite similar (24-h DTS $58.6 \pm 6$ l s$^{-1}$; Cl$^-$ $72.8 \pm 0.1$ l s$^{-1}$, Ca$^{2+}$ $68.8 \pm 0.2$ l s$^{-1}$; RWT $67.0 \pm 20$ l s$^{-1}$) with a mean of $66.8$ l s$^{-1}$. Differential gauging failed to characterize this small (5%) input due to a level of uncertainty that exceeded the inflow size, and this uncertainty seemed to be underestimated using the ISO and USGS statistical uncertainty analyses. Non-ideal field conditions over most stream cross-sections caused by high turbulence, velocity, macrophyte growth and variable bedform influenced observed error and may be avoided in other systems. The RWT dilution captured the focused groundwater inflow accurately in this study, but the estimate was less precise and indicated this method would be insensitive to inflows less than 20 l s$^{-1}$, although this precision could be improved with higher tracer plateau concentrations.

Changes in stream chemistry were used in two end-member mixing models for both Cl$^-$ and Ca$^{2+}$ because the ratio–ratio plot of Cl : Na and Ca : Na in mixed stream water yielded a linear relationship, indicating two well defined end-members. The abrupt change in stream chemistry around the focused input was easily identified and used to determine a precise estimate of groundwater inflow, but the samples taken directly below this input were variable due to mixing noise captured by the instantaneous point measurements. A more diffuse inflow

of groundwater (12.0 l s$^{-1}$) over a 75-m reach leading up to the focused input was described by chemical analysis, but indistinguishable with the DTS and RWT data. Such small, diffuse groundwater inflows can be identified with the end-member mixing, given the high precision of the method based on the sensitivity analysis, which indicated inflows as small as 0.1 l s$^{-1}$ could be quantified under these site-specific conditions. The chemical makeup of the local groundwater was highly variable with depth and location, and water collected from shallow piezometers within the stream bank were used for this analysis in part because they fell along the stream mixing line of the ratio–ratio plot. Some deeper wells with higher saline concentrations had the same ratios but would have greatly underestimated inflow if applied to the mixing models, suggesting caution must be used when selecting the groundwater end member from local wells. In this case the stream bank seep was an obvious place to install piezometers, but in more ambiguous settings heat tracing or very high resolution water sampling may be necessary to identify areas from which to sample groundwater reliably.

DTS data had the highest spatial resolution (1.5 m) and allowed for the direct identification of the focused groundwater seep. A curve fit to the return of stream water to ambient temperature allowed both an estimate of the spring's downstream temperature influence ($\sim$400 m) and identification of unmixed groundwater inputs, which corresponded with the exact location of springs. Overall, mixing of stream and groundwater in close proximity to the inflow was best characterized by the DTS, as data were integrated over time in contrast to the instantaneous chemical and RWT samples. Absolute groundwater inflow estimates were sensitive to time of day and integration time, which likely affected the 24-h mean method. Times of fast stream temperature change provided poorer estimates of groundwater inflow, especially when solar input was at a peak and the stream was warmed differentially and the cable may have been affected by heat conduction from the sediments. Estimates made over 2-h periods, when direct solar input was low and overall stream temperature was changing slowly, generated groundwater inflow estimates that were most similar to the other methods ($69.9 \pm 6$ l s$^{-1}$ and $63.7 \pm 6$ l s$^{-1}$). Even during optimal times of day, data integration times of several hours may be necessary to reduce error introduced by systematic noise in the temperature signal.

The use of ambient tracers such as heat and geochemistry for mixing models is viable in part because they provide direct information regarding groundwater inflows, and these tracers should be at relative steady state assuming stream discharge change is slow temporally. We have shown that geochemical analysis can be very effective when the chemistry of surface and groundwater differ, as may be case for groundwater contamination. Further, when the groundwater temperature differs from stream water, DTS data can provide similar estimates of focused groundwater inflow to the chemical data but provides a finer spatial characterization of inflow distribution. Even

if groundwater temperatures are similar to the stream, inflows may also be identified as areas of lower diurnal stream temperature variance influenced by the constant temperature groundwater source. Although the cost of a DTS unit may be a prohibitive, they may be rented or borrowed from a variety of sources (e.g. Tyler and Selker, 2009), and the fibre-optic cables themselves are relatively affordable and may be viewed as a consumable of the installation. Once the cable is installed, a spatially and temporally continuous and extensive data-set can be collected at varied flow and climate conditions, moving stream research beyond the point measurement limits and allowing focused-source contaminant loading to be better quantified. In summary, distributed temperature data can be used to estimate groundwater inflow magnitude in a comparable manner to more conventional methods, and describes inflow distribution at higher spatial resolution, even modest inputs to large streams.

## REFERENCES

Anderson MP. 2005. Heat as a ground water tracer. *Ground Water* **43**: 951–968.

Auer M, Effler S, Storey M, Connors S, Sze P. 1996. Biology. In *Limnological and Engineering Analysis of a Polluted Urban Lake: Prelude to Environmental Management of Onondaga Lake, New York,* Effler S (ed). Springer-Verlag: New York, NY; 384–534.

Brunke M, Gonser T. 1997. The ecological significance of exchange processes between rivers and groundwater. *Freshwater Biology* **37**: 1–33.

Carter RW, Davidian J. 1968. General procedure for gaging streams, U.S. Geological Survey, Techniques for Water-Resources Investigations, Book 3, Chapter A-6.

Christensen TH, Kjeldsen P, Bjerg PL, Jensen DL, Christensen JB, Baun A, Albrechtsen HJ, Heron C. 2001. Biogeochemistry of landfill leachate plumes. *Applied Geochemistry* **16**: 659–718.

Constantz J. 1998. Interaction between stream temperature, streamflow, and groundwater exchanges in Alpine streams. *Water Resources Research* **34**(7): 1609–1615.

Dakin JP, Pratt DJ, Bibby GW, Ross J. 1985. Distributed optical fiber Raman temperature sensor using a semiconductor light-source and detector. *Electronics Letters* **21**: 569–570. DOI:10·1049/el:19850402.

Effler S, Whitehead K. 1996. Tributaries and Discharges. In *Limnological and Engineering Analysis of a Polluted Urban Lake: Prelude to Environmental Management of Onondaga Lake, New York,* Effler S (ed). Springer-Verlag: New York, NY; 97–199.

Fulford JM. 2001. Accuracy and consistency of water-current meters. *Journal of the American Water Resources Association* **37**: 1215–1224.

Grattan KTV, Sun T. 2000. Fiber optic sensor technology: an overview. *Sensors and Actuators A: Physical* **82**(1–3): 40–61. DOI:10·1016/S0924-4247(99)00368-4

Harvey JW, Wagner BJ. 2000. Quantifying hydrologic interactions between streams and their subsurface hyporheic zones. In *Streams and*

Ground Waters, Jones JB, Mulholland PJ (eds). Academic Press: San Diego, CA.

Hatch CE, Fisher AT, Revenaugh JS, Constantz J, Ruehl C. 2006. Quantifying surface water-groundwater interactions using time series analysis of streambed thermal records: Method development. *Water Resources Research* **42**: W10410. DOI: 10·1029/2005WR004787.

Kalbus E, Reinstorf F, Schirmer M. 2006. Measuring methods for groundwater-surface water interactions: A review. *Hydrology and Earth System Sciences* **10**: 873–887.

Kasnavia T, Vu D, Sabatini DA. 1999. Fluorescent dye and media properties affecting sorption and tracer selection. *Ground Water* **37**: 376–381.

Keery J, Binley A, Crook N, Smith JWN. 2007. Temporal and spatial variability of groundwater-surface water fluxes: Development and application of an analytical method using temperature time series. *Journal of Hydrology* **336**: 1–16.

Kilpatrick FA, Cobb ED. 1985. Measurement of discharge using tracers, US Geological Survey Techniques of Water-resources Investigations, Book 3, Chapter A16·52.

Kobayashi D. 1985. Separation of the snowmelt hydrograph by stream temperatures. *Journal of Hydrology* **76**: 155–162.

Land M, Ingri J, Andersson PS, Ohlander B. 2000. Ba/Sr, Ca/Sr and Sr-87/Sr-86 ratios in soil water and groundwater: Implications for relative contributions to stream water discharge. *Applied Geochemistry* **15**: 311–325.

Langmuir CH, Vocke JRD, Hanson GN, Hart SR. 1978. A general mixing equation with applications in icelandic basalts. *Earth and Planetary Science Letters* **37**: 380–392.

Loheide SP II, Gorelick SM. 2006. Quantifying stream-aquifer interactions through the analysis of remotely sensed thermographic profiles and in situ temperature histories. *Environmental Science and Technology*, **40**: 3336–3341. DOI:10·1021/es0522074.

Lowry CS, Walker JF, Hunt RJ, Anderson MP. 2007. Identifying spatial variability of groundwater discharge in a wetland stream using a distributed temperature sensor. *Water Resources Research* **43**: W10408. DOI:10·1029/2007wr006145.

Matthews DA, Effler SW. 2003. Decreases in pollutant loading from residual soda ash production waste. *Water Air and Soil Pollution* **146**: 55–73.

Moffett KB, Tyler SW, Torgersen T, Menon M, Selker JS, Gorelick SM. 2008. Processes controlling the thermal regime of saltmarsh channel beds. *Environmental Science & Technology* **42**: 671–676. DOI:10·1021/Es071309m.

Neilson B, Hatch C, Ban H, Tyler S. 2010. Solar radiative heating of fiber optic cables used to monitor temperatures in water. *Water Resources Research*. **46**: W08540, DOI: 10·1029/2009WRR008354.

Panno SV, Hackley KC, Hwang HH, Greenberg SE, Krapac IG, Landsberger S, O'Kelly DJ. 2006. Characterization and identification of na-cl sources om ground water. *Ground Water* **44**: 176–187.

Payn RA, Gooseff MN, McGlynn BL, Bencala KE, Wondzell SM. 2009. Channel water balance and exchange with subsurface flow along a mountain headwater stream in Montana, USA. *Water Resources Research* **45**: W11427. DOI:10·1029/2008WR007644

Robson A, Neal C. 1990. Hydrograph separation using chemical techniques—an application to catchments in mid-wales. *Journal of Hydrology* **116**: 345–363.

Schmadel NM, Neilson BT, Stevens DK. 2010. Approaches to estimate uncertainty in longitudinal channel water balances. *Journal of Hydrology* **394**: 357–369. DOI:10·1016/j.jhydrol.2010·09·011.

Selker J, Giesen NVD, Westhoff M, Luxemburg W, Parlange MB. 2006a. Fiber optics opens window on stream dynamics. *Geophysical Research Letters* **33**: L24401.

Selker JS, Thevenaz L, Huwald H, Mallet A, Luxemburg W, de Giesen NV, Stejskal M, Zeman J, Westhoff M, Parlange MB. 2006b. Distributed fiber-optic temperature sensing for hydrologic systems. *Water Resources Research* **42**: W12202.

SonTek/YSI. 2009. Flowtracker handheld ADV technical manual, Firmware version 3·7. SonTek/YSI, Division of YSI Inc. San Diego, CA, USA.

Soupir ML, Mostaghimi S, Mitchem C. 2009. A comparative study of stream-gaging techniques for low-flow measurements in two virginia tributaries. *Journal of the American Water Resources Association* **45**: 110–122. DOI:10·1111/J.1752-1688·2008·00264.X.

Thoreau HD. 1854. *Walden; or, Life in the Woods*. Boston: Ticknor & Fields.

Tyler S, Selker J. 2009. New user facility for environmental sensing. *Eos* **90**: 483.

Tyler SW, Selker JS, Hausner MB, Hatch CE, Torgersen T, Thodal CE, Schladow SG. 2009. Environmental temperature sensing using raman

spectra dts fiber-optic methods. *Water Resources Research* **45**: W00D23. DOI:10·1029/2008wr007052.

Westhoff MC, Savenije HHG, Luxemburg WMJ, Stelling GS, van de Giesen NC, Selker JS, Pfister L, Uhlenbrook S. 2007. A distributed stream temperature model using high resolution temperature observations. *Hydrology and Earth System Sciences* **11**: 1469–1480.

Whittemore DO. 2007. Fate and identification of oil-brine contamination in different hydrogeologic settings. *Applied Geochemistry* **22**: 2099–2114. DOI: 10·1016/J.Apgeochem.2007·04·002.

Zellweger GW. 1994. Testing and comparison of 4 ionic tracers to measure stream-flow loss by multiple tracer injection. *Hydrological Processes* **8**: 155–165.